

Articles

Pressure-Induced Dissociation of Fluorescein from the Anti-Fluorescein Single-Chain Antibody 4-4-20[†]

Tatiana Coelho-Sampaio and Edward W. Voss, Jr.*

Department of Microbiology, University of Illinois, 131 Burrill Hall, 407 South Goodwin Avenue, Urbana, Illinois 61801

Received July 8, 1993*

ABSTRACT: Hydrostatic pressure was used to dissociate fluorescein (Fl) from the high-affinity anti-Fl single-chain antibody 4-4-20 (SCA 4-4-20). Fl dissociation was monitored by measuring (1) the shift in the Fl absorption peak, (2) the recovery in Fl fluorescence intensity, which is quenched upon SCA binding, or (3) the decrease in Fl fluorescence polarization. Pressure effects were studied at two different Fl:SCA 4-4-20 molar ratios: 1:1, at which Fl fluorescence quenching was ca. 35% at atmospheric pressure, and 1:5, at which quenching reached 95–97% under the same conditions. In both cases, pressure-induced dissociation was favored by concomitant dilution of protein and ligand. Dissociation constants (K_D) at each pressure were calculated on the basis of measurements of Fl fluorescence polarization under pressure. The dependence of K_D , and consequently of ΔG of dissociation, on pressure permitted calculation of the magnitude of the standard volume change (ΔV) involved in the dissociation process. According to this study, ΔV of dissociation for the Fl–SCA complex is –50 mL/mol, which corresponds to a 10-times higher value than that found for dissociation of Fl from the intact IgG mAb 4-4-20 [Herron, J. N., Kranz, D. M., Jameson, D. M., & Voss, E. W., Jr. (1986) *Biochemistry* 25, 4602–4609]. This difference is explained in terms of a higher overall flexibility of unliganded SCA and of a less stable binding site in SCA relative to mAb. This interpretation was based on the findings that the Fl ligand stabilizes SCA conformation, that Fl dissociation was not determined by primary conformational changes in SCA structure induced by hydrostatic pressure, and that Fl is more accessible to the charged quencher iodide when liganded to SCA than when bound to mAb. Finally, the strong temperature dependence for pressure-induced dissociation of Fl from SCA 4-4-20 combined with the fact that association of the Fl hapten to SCA was found to be enthalpically unfavorable indicates that formation of the Fl–SCA 4-4-20 complex is an entropy-driven process.

Single-chain antibody 4-4-20 (SCA 4-4-20)[†] is a genetically engineered derivative of the high-affinity anti-Fl mAb 4-4-20 (Bird et al., 1988; Bedzyk et al., 1990). The SCA molecule is comprised of the two variable domains, V_L and V_H , of the corresponding mAb joined covalently by a short peptide linker (Huston et al., 1988; Bird et al., 1988; Chaudhary et al., 1989;

Glockshuber et al., 1990). The relatively flexible linker was designed to allow independent folding of the two variable domains necessary to preserve the high-affinity antigen recognition function (Bird et al., 1988; Bedzyk et al., 1990). SCA molecules present specific advantages over mAbs. For instance, SCA is efficiently cleared from the circulation, which makes it more convenient than mAbs for use in *in vivo* imaging and tumor therapeutics (Bird et al., 1988; Yokota et al., 1992). Furthermore, SCA molecules allow the structure–function study of the immunoglobulin variable domains independent of the constant regions and, because of their expression in bacteria, facilitate site-direct mutagenesis (Denzin et al., 1991).

[†] This work was supported by a grant from the Biotechnology Research Development Corp., Peoria, IL.

* To whom correspondence should be addressed.

• Abstract published in *Advance ACS Abstracts*, September 15, 1993.

[†] Abbreviations: Fl, fluorescein; SCA, single-chain antibody; mAb, monoclonal antibody; V_L , light-chain variable region; V_H , heavy-chain variable region; IgG, immunoglobulin G.

Despite broad interest in the use of SCA, little has been done on characterization of the molecular basis of antigen binding by SCA molecules as well as on definition of thermodynamic parameters involved in this interaction. Hydrostatic pressure is now established as a valuable tool in the study of interactions between protein subunits (Paladini & Weber, 1981; Thompson & Lakowicz, 1984; Silva et al., 1986; Coelho-Sampaio et al., 1991) and between proteins and ligands (Li et al., 1976a; Masson & Balny, 1990; Ronzani et al., 1991). Using hydrostatic pressure, it is possible to derive information regarding the thermodynamics of biological processes under isothermal conditions (Weber & Drickamer, 1983; Weber, 1987, 1992). The effects of pressure on immunoglobulins have been previously studied using the Bence-Jones protein Mcg (Herron et al., 1985), bovine IgG (Howlett et al., 1992), and the anti-fluorescein Mabs 4-4-20, 20-19-1, and 20-20-3 (Herron et al., 1986). Collectively these reports have shown that pressure applied up to 3 kbar does not promote changes either in the secondary or in the tertiary structures of the IgGs but interferes with the quaternary arrangement of the two light chains that comprise the Bence-Jones protein Mcg. Furthermore, pressure promotes a limited dissociation of ligands from both Mcg and anti-FI Mabs.

In this work, we systematically studied the pressure-induced dissociation of bound fluorescein from SCA 4-4-20. Ligand dissociation was monitored by taking advantage of the significant spectroscopic changes exhibited by the fluorescein hapten upon specific binding to antibody (Kranz & Voss, 1981; Kranz et al., 1983). We demonstrate that the FI-SCA complex is significantly more sensitive to pressure-induced dissociation than the FI-mAb complex, which correlates with a large difference in volume changes involved in dissociation of each complex. We also report the effects of temperature and protein concentration on the dissociation process. The aim of the studies was to gain additional information regarding the molecular basis of the FI-SCA interactions in order to correlate the thermodynamic properties involved in binding of FI to SCA and intact immunoglobulins.

MATERIALS AND METHODS

Single-Chain Antibody 4-4-20. SCA was constructed and expressed as described elsewhere (Bird et al., 1988; Denzin et al., 1991). Isolation of SCA was obtained by extracting inclusion bodies accumulated in *Escherichia coli* cells. Briefly, protein aggregates were denatured in 6 M guanidine hydrochloride in 50 mM Tris-HCl, pH 8.0, 10 mM CaCl₂, 100 mM KCl, and 0.1 mM phenylmethanesulfonyl fluoride. The solubilized protein was refolded by a slow dilution (1:1000) in refolding buffer (50 mM Tris-HCl, pH 8.0, 10 mM CaCl₂, 50 mM KCl, and 0.1 mM phenylmethanesulfonyl fluoride) at room temperature. SCA was concentrated by successive filtration steps followed by affinity purification using FI-Sepharose 4B.

Monoclonal Antibody 4-4-20. Mab 4-4-20 was obtained from mouse ascites fluid by affinity purification using FI-Sepharose 4B as previously described (Kranz & Voss, 1981; Reinitz & Voss, 1984).

Hydrostatic Pressure Experiments. Hydrostatic pressure in the range of 1 bar to 2.4 kbar was achieved using the pressure cell described by Paladini and Weber (1981). Fluorescence polarization values measured in the pressure bomb were corrected for birefringence of the quartz windows as described by Paladini and Weber (1981). Protein samples prepared in 10 mM Tris-HCl buffer, pH 8.0, were stabilized for 2 min at each pressure before measurements, and, unless otherwise indicated, experiments were performed at 25 °C.

Fluorescence measurements at -16 °C were performed in aqueous medium as follows. Pressure was increased to 2.4 kbar at 3 °C, and spectra were recorded at 200-bar increments. Pressure was then released to 1 kbar and reversibility verified. Under 1-kbar pressure, the samples were cooled to -16 °C, and the pressure was again raised incrementally to 2.4 kbar.

Absorption Spectra. Absorption measurements were performed at 25 °C using an SLM-Aminco 3000 spectrophotometer, adapted to hold the pressure bomb.

Fluorescence Measurements. Steady-state fluorescence spectra and polarization were measured using an ISS (Champaign, IL) GREG-PC spectrofluorometer. The reported FI fluorescence intensities correspond to the integrated area of the emission spectra at each pressure calculated as $\int I(\lambda) d\lambda$, where λ is the emission wavelength (in nanometers) and $I(\lambda)$ is the fluorescence intensity at a given wavelength. In FI fluorescence measurements, the excitation wavelength was 485 nm, and the emission was either scanned from 500 to 600 nm (for spectra) or fixed at 525 nm (for polarization). In intrinsic SCA fluorescence measurements, excitation was at 275 nm, emission was recorded between 310 and 450 nm, and the reported intensities correspond to the fluorescence intensities at the emission peak (349 nm). In the measurements of the intrinsic fluorescence of SCA in the presence of fluorescein, the raw data obtained were corrected for energy transfer from tryptophan to fluorescein. Appropriate corrections were made as follows. The degrees of FI dissociation (α) based on FI fluorescence polarization data (see description of Figure 4) were obtained at various dilutions of FI at a fixed SCA concentration. Quenching of the intrinsic fluorescence (due to energy transfer to FI) was also measured at each dilution. The plot of intrinsic fluorescence quenching against α was linear, which allowed prediction of quenching at each value of α . Values of α at each pressure were based on fluorescence polarization measurements.

Iodide Quenching. Iodide quenching of FI was assayed by measuring the decrease in the total fluorescence emission at 520 nm when small volumes of freshly prepared concentrated stock solution of potassium iodide were added to the cuvette. Intensities were corrected for the dilution caused by addition of quencher.

RESULTS

Effect of Hydrostatic Pressure on Absorption and Fluorescence Emission Spectra of FI SCA 4-4-20. The effects of hydrostatic pressure on the maximal absorption peak (Abs_{max}) and on the total fluorescence intensity of fluorescein are shown in Figure 1. The concentration of FI in the experiments was 1.8 μ M, which was the minimal FI concentration allowable to resolve the peaks of Abs_{max} . The FI:SCA molar ratio was 1:1, which promoted only partial binding (ca. 35%) of the total FI present. When hydrostatic pressure was increased incrementally from 1 bar to 2.4 kbar, the FI Abs_{max} shifted from 499.8 to 497.6 nm (Figure 1, open circles). This blue-shift is compatible with an increase in the fraction of free FI relative to bound FI, whose Abs_{max} are 492 and 505 nm, respectively (Kranz et al., 1982).

Measurements of the fluorescence emission of fluorescein also suggested dissociation of FI from SCA 4-4-20 upon application of pressure (Figure 1, closed circles). At atmospheric pressure, addition of SCA 4-4-20 promoted a 35% decrease in the fluorescence intensity of fluorescein. At 2.4 kbar, a partial recovery of the initial fluorescence from 65% to 71% was obtained, indicating that FI was released from the 4-4-20 binding site. The pressure-induced blue-shift in

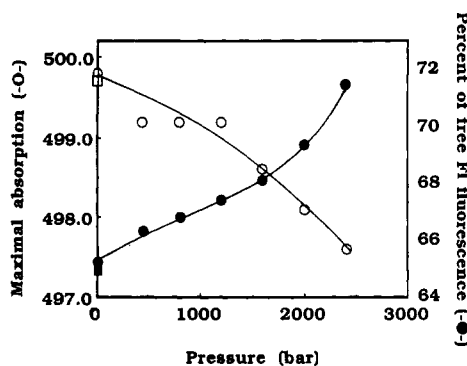


FIGURE 1: Effect of pressure on FI absorption spectra and on FI fluorescence emission. Absorption and fluorescence spectra of 1.8 μM FI in the presence of 1.8 μM SCA 4-4-20 were measured as described under Materials and Methods. Maximal absorption wavelengths at each pressure are shown (O). Fluorescence data were normalized for the area (total emission intensity) of the fluorescence spectrum of FI in the absence of SCA 4-4-20 (●). The values found for the maximal absorption peak and the percent of free FI fluorescence at atmospheric pressure after release of pressure are also shown (□ and ■, respectively).

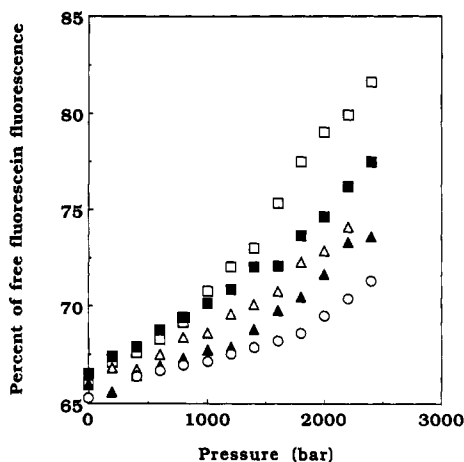


FIGURE 2: Pressure-induced FI fluorescence increase depends on FI and SCA 4-4-20 concentrations (molar ratio of 1:1). Concentrations of FI at each experiment were 1.8 (O), 0.6 (▲), 0.2 (Δ), 0.1 (■), and 0.05 μM (□). In all cases, the FI:SCA 4-4-20 molar ratio was kept constant at 1:1, which promoted 33–35% FI fluorescence quenching at atmospheric pressure.

absorption and the recovery of quenched fluorescence were both reversible upon release of pressure (Figure 1, open and closed squares, respectively).

Pressure-Induced Fluorescence Quenching at Different SCA 4-4-20 Concentrations. The effects of increasing hydrostatic pressure on FI fluorescence emission were assayed at five different SCA concentrations ranging from 0.05 to 1.8 μM but retaining the 1:1 molar ratio of FI to SCA at each concentration (Figure 2). Decrease in protein concentration increased the recovery of FI fluorescence intensity induced by pressure (Figure 2). The protein concentration dependence corroborates the interpretation that pressure induces dissociation of FI from SCA 4-4-20, since a first-order process, such as conformational rearrangements at the FI binding site, should be independent of concentration (Weber, 1987).

Figure 3 shows the dependence of pressure-induced dissociation on protein concentration when the FI:SCA 4-4-20 ratio was 1:5. At this ratio (i.e., excess protein), the remaining FI fluorescence upon SCA binding at atmospheric pressure changed from 65% (Figures 1 and 2) to 3% (Figure 3). An increase in pressure up to 2.4 kbar did not affect fluorescence intensity when the concentration of SCA was 4.2 μM (Figure

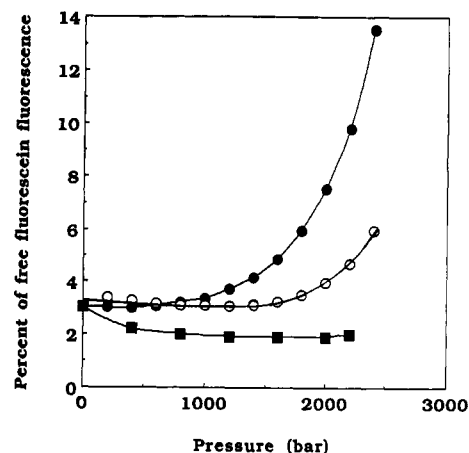


FIGURE 3: Pressure-induced FI fluorescence increase depends on FI and SCA 4-4-20 concentrations (molar ratio of 1:5). Concentrations of FI at each experiment were 0.8 (■), 0.1 (O), and 0.02 μM (●). In all cases, the FI:SCA 4-4-20 molar ratio was kept constant at 1:5, which promoted 95–97% FI fluorescence quenching at atmospheric pressure.

3, squares). At this concentration, even a slight decrease in fluorescence was observed, which might result from small changes in the position of the quartz windows of the bomb upon increasing pressure. At 0.5 μM SCA 4-4-20, dissociation occurred at pressures greater than 1.6 kbar, and the maximal recovery obtained at 2.4 kbar was 6% of the free FI fluorescence (Figure 3, open circles). When the SCA concentration was decreased to 0.1 μM , dissociation started at 1 kbar and reached a maximal recovery of 14% at 2.4 kbar (Figure 3, closed circles). It is interesting to note that under this last condition (0.5 μM SCA 4-4-20 and 0.02 μM FI) the resolvability of the fluorescence increments induced by pressure was improved, since the net increases measured in fluorescence emission were higher than 4 times (3–14%, corresponding to increases in raw spectral areas typically from 100 000 to 450 000 fluorescence arbitrary units).

Effect of Pressure on FI Fluorescence Polarization. Binding of FI to anti-FI antibodies is followed by a pronounced increase in the steady-state fluorescence polarization of the hapten, which correlates with an increased restriction of the ligand's mobility (Herron et al., 1984, 1986). Because of this correlation, FI polarization was measured to follow the pressure-induced dissociation of FI from SCA 4-4-20 (Figure 4). The effect of pressure on fluorescence anisotropy, r [calculated as $r = 2P/(3 - P)$ where P is the polarization] is shown in Figure 4A. The profile obtained differs significantly from that observed measuring FI fluorescence intensity under the same conditions (compare to Figure 3, closed circles). This difference is explained by the fact that the two species involved in the equilibrium of dissociation, FI bound and FI free, have significantly different quantum yields. Therefore, the contribution of free FI (which has a ~25 times higher quantum yield) to the average anisotropy will be much greater than the contribution of bound fluorescein. To correct for the difference in quantum yields, the polarization data of Figure 4A were replotted in terms of the degree of dissociation (α_p) at each increment of pressure (Paladini & Weber, 1981), calculated as

$$\alpha_p = [1 + Q(r_p - r_F)/(r_B - r_p)]^{-1} \quad (1)$$

where Q is the ratio of the fluorescence quantum yields of free and bound forms, r_p is the anisotropy at each pressure, and r_F and r_B are the anisotropies for free and bound states, respectively.

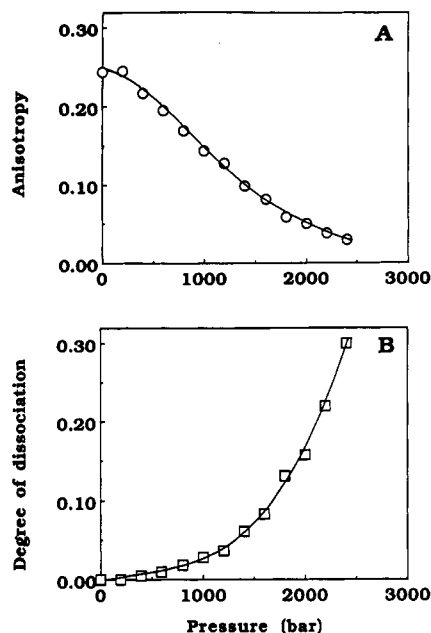


FIGURE 4: Effect of pressure on FI fluorescence anisotropy. Fluorescence anisotropy of 0.02 μ M FI in the presence of 0.1 μ M SCA was measured at 25 $^{\circ}$ C at increasing pressure (panel A). Data were replotted in terms of the degree of dissociation as described under Results (panel B).

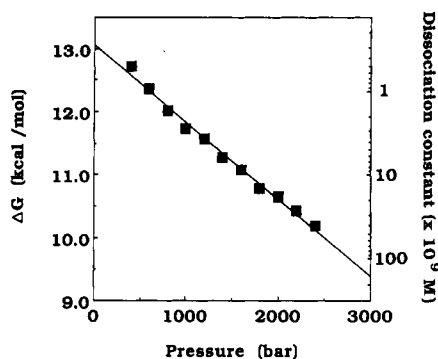


FIGURE 5: Dependence of ΔG_{diss} on hydrostatic pressure. Values for ΔG_{diss} were calculated as described under Results, based on the change in the degree of dissociation with pressure shown in Figure 4. The straight line was fitted to data points by linear regression.

The plot of α_p versus pressure (Figure 4B) presents a similar profile to that observed when fluorescence intensities were measured (compare with Figure 3, closed circles). At a pressure of 2.4 kbar, the degree of dissociation was 0.3.

Knowledge of the degrees of ligand dissociation permitted calculation of the dissociation constants (K_D) at each pressure using the equation:

$$K_D = \{\alpha_p([SCA]_0 - [FI]_0 - \alpha_p[FI]_0)\} / (1 - \alpha_p) \quad (2)$$

where $[SCA]_0$ and $[FI]_0$ are the total concentrations of SCA 4-4-20 and FI, respectively.

The dissociation constants relate to the free energy of dissociation, ΔG_{diss} , as $\Delta G_{\text{diss}} = -RT \ln K_D$, where R and T have the usual meanings. Values of ΔG_{diss} decreased from 13 to 10 kcal/mol upon increasing the hydrostatic pressure from 1 bar to 2.4 kbar (Figure 5), indicating that the affinity of SCA 4-4-20 for FI decrease *ca.* 10^3 times in this pressure range. The dissociation constant at atmospheric pressure is given by the y -axis intercept in Figure 5. The value found was 2.7×10^{-10} M, which corresponds to a K_a of 3.7×10^9 M $^{-1}$. The latter value is in good agreement with the previously

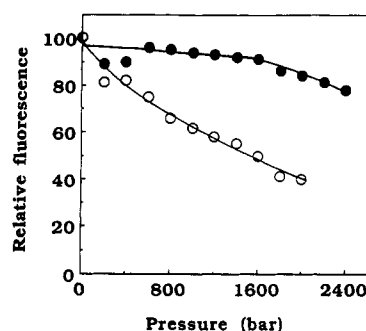


FIGURE 6: Effect of pressure on intrinsic SCA 4-4-20 fluorescence. Pressure effects on SCA 4-4-20 are shown in the absence (O) and in the presence of FI (●). The y axis shows the percent of change in intrinsic fluorescence intensity upon application of pressure, relative to the intensity at atmospheric pressure. Typical values for the intensities at atmospheric pressure (100%) were 23 000 and 16 000 AU in the absence and in the presence of FI, respectively. Corrections for FI quenching of intrinsic fluorescence were performed as described under Materials and Methods.

reported K_a of 5×10^9 M $^{-1}$ for the FI-SCA 4-4-20 complex (Bedzyk et al., 1990).

The standard volume change upon dissociation (ΔV_{diss}) was calculated as

$$\Delta V = (\partial \Delta G_{\text{diss}} / \partial p)_T \quad (3)$$

From the slope of the plot ΔG vs pressure (Figure 5), a $\Delta V_{\text{diss}} = -50.7$ mL/mol was calculated. This value is 10 times higher than that reported for the dissociation of FI from mAb 4-4-20, which was in the range of 5 mL/mol (Herron et al., 1986).

Effect of Pressure on the Intrinsic Fluorescence. In order to study possible effects of pressure on SCA 4-4-20 structure, the intrinsic fluorescence of the tryptophan residues of SCA was measured upon increasing hydrostatic pressure (Figure 6). In the nonliganded protein, pressure promotes a decrease in SCA intrinsic fluorescence (Figure 6, open circles), indicating that the antibody undergoes conformational changes associated with pressure increase. Protein conformational changes associated with increased exposure of tryptophan residues to the aqueous medium are generally accompanied by red-shifts in the intrinsic fluorescence emission spectra (Lakowicz, 1983). The decreased fluorescence intensity shown in Figure 6 (open circles) did not correlate with red-shifts in the spectra (not shown), indicating that tryptophan residues were not being further exposed to water under pressure.

When hydrostatic pressure was applied to liganded SCA (Figure 6, closed circles), the decrease in fluorescence intensity was much less pronounced than in the absence of ligand. In fact, fluorescence intensities remained essentially unchanged up to 1.6 kbar. This result suggested that in the range of 1.0–1.6 kbar, pressure promoted FI dissociation (Figures 3 and 4) but did not significantly affect the overall structure of the SCA molecule in the liganded state. Furthermore, comparison between the effects of pressure on the liganded and nonliganded states (Figure 6, open and closed circles) suggested that FI stabilizes the structure of SCA 4-4-20 against pressure perturbation.

Iodide Quenching of FI Fluorescence. The accessibility of the FI hapten in the binding sites of SCA and mAb 4-4-20 was studied by measuring iodide quenching of bound FI. This experiment was performed in order to search for eventual differences at the level of the binding sites between SCA and mAb 4-4-20 that could account for the large difference in the ΔV_{diss} of FI from each antibody molecule (Figure 5). The Stern-Volmer plots for iodide quenching are shown in Figure 7. Addition of increasing amounts of iodide did not affect the

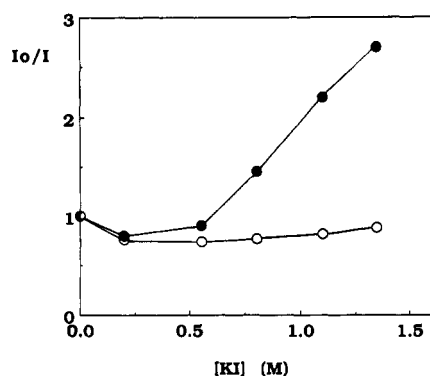


FIGURE 7: Iodide quenching of FI fluorescence. Iodide quenching of FI bound to either mAb (O) or SCA 4-4-20 (●) was measured at 25 °C as described under Materials and Methods. The concentrations of FI, SCA, and mAb were 0.02, 0.1, and 0.05 μ M, respectively.

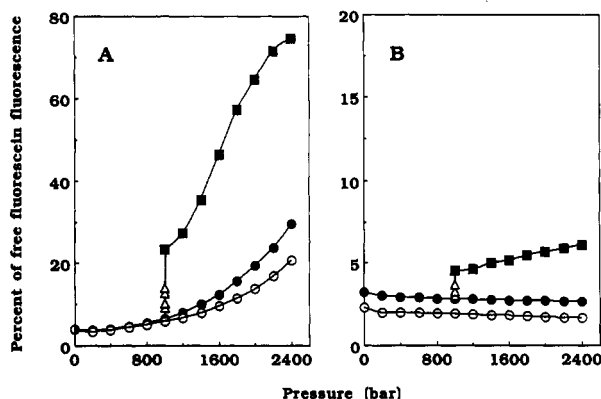


FIGURE 8: Effect of temperature on pressure-induced dissociation of FI. Pressure-induced dissociation of FI from SCA (panel A) or from mAb 4-4-20 (panel B) was measured at 25 (O), 3 (●), and -16 °C (■). Concentrations of FI, SCA, and mAb were 0.02, 0.1, and 0.05 μ M, respectively. The effect of decreasing temperature from 3 to -16 °C on FI dissociation at 1 kbar is also shown (Δ).

fluorescence emission of FI bound to mAb 4-4-20 (open circles), indicating that FI is inaccessible to iodide when bound to the mAb molecule. In fact, a small increase in the fluorescence emission at low iodide concentrations was observed. This effect has been previously observed by Swindlehurst and Voss (1991) in both steady-state and lifetime fluorescence analyses of FI bound to mAb 4-4-20.

When iodide was added to the FI-SCA 4-4-20 complex, extensive quenching of FI fluorescence was observed (Figure 7, closed circles). This result indicates that FI is more accessible to iodide in the SCA binding site than in mAb site.

Effects of Temperature on Pressure-Induced Dissociation of FI. Pressure-induced dissociation of FI from SCA 4-4-20 or from mAb 4-4-20 was studied as a function of temperature (Figure 8, panels A and B, respectively). A decrease in temperature from 25 to 3 °C facilitated dissociation of FI from SCA, which reached 30% at the lower temperature (compare closed and open circles in panel A). At 1 kbar, a decrease in temperature from 3 to -16 °C promoted release of FI from the binding site (open triangles). At -16 °C, ligand dissociation was extremely sensitive to pressure, leading to a FI fluorescence recovery of about 80% at 2.4 kbar.

The FI-mAb 4-4-20 complex did not dissociate under pressure up to 2.4 kbar either at 25 or at 3 °C (Figure 8B, open circles and closed circles). A decrease in temperature from 3 to -16 °C at 1 kbar promoted FI dissociation from the mAb (triangles). At -16 °C, an increase in pressure from 1 to 2.4 kbar promoted an increase in the recovery of the quenching of FI fluorescence from 4.5 to 6.5%.

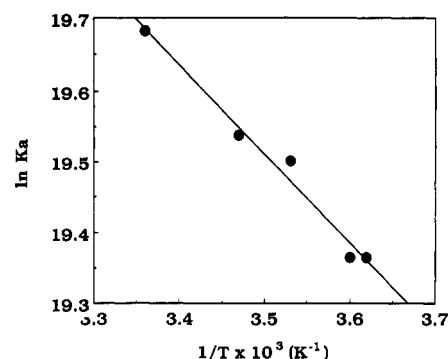


FIGURE 9: van't Hoff plot for FI binding to SCA 4-4-20. The fractions of bound FI were measured upon temperature decrease from 25 to 3 °C. Association constants (K_a) were calculated as described under Results.

Temperature-Induced FI Dissociation. The strong temperature dependence of pressure-induced FI dissociation from SCA 4-4-20 (Figure 8) suggested that the balance between entropic and enthalpic components involved in the formation of the FI-SCA complex could be different as compared to the balance of these thermodynamic parameters that characterize formation of the FI-mAb complex (Herron et al., 1986). In order to further explore this possibility, FI dissociation from SCA 4-4-20 was measured as a function of temperature at atmospheric pressure. Figure 9 shows the van't Hoff plot obtained in the temperature range from 3 to 25 °C, where association constants (K_a) were calculated from the degrees of dissociation obtained at each temperature as described by Li et al. (1976a,b). Using $\Delta H = RT^2(\partial \ln K_a / \partial T)_P$, ΔH_{assn} values were calculated to be between 2.3 and 2.6 kcal/mol in the range of temperatures assayed. The positive ΔH of association indicates that binding of FI to SCA 4-4-20 is an enthalpically unfavorable process, in contrast with what has been shown for the association of FI to mAb 4-4-20 (Herron et al., 1986). In the same temperature range, an entropy change for the association of FI with SCA 4-4-20 (ΔS_{assn}) of 47 cal/kmol was calculated from $\Delta G = \Delta H - T\Delta S$.

DISCUSSION

Hydrostatic pressure promoted dissociation of FI from the anti-FI SCA 4-4-20. This conclusion is based on the facts that (1) pressure shifted the absorption peak of FI toward the value observed for free FI (Figure 1), (2) pressure reversed the quenching of FI fluorescence that occurs upon binding of FI to anti-FI antibodies (Figures 1-3), and (3) the effects of pressure were shown to be dependent on protein concentration (Figures 2 and 3). When the FI:SCA molar ratio was 1:5, pressure-induced changes in fluorescence presented a plateau at low pressures, whose extension was dependent on protein concentration (Figure 3). When the ratio was 1:1 (Figures 1 and 2), this plateau was not evident. Instead, a biphasic profile was observed. Under the latter condition, a significant amount of FI was not bound to SCA 4-4-20 as indicated by the fact that only 35% of FI fluorescence was quenched at atmospheric pressure. We have observed that pressure promotes an increase in the fluorescence emission of FI in the absence of antibody (not shown). Thus, the first component of dissociation curves at the molar ratio 1:1 may be associated with the effect of pressure on unbound FI.

Pressure-induced dissociation was further confirmed by measuring FI fluorescence polarization. The degree of dissociation observed at 2.4 kbar was 0.3 (Figure 4B). This value was slightly higher than expected by comparison with fluorescence intensity measurements which reported a recovery

of 14% of FI fluorescence. This difference may be attributable to the constant light-scattering distortion caused by the pressure bomb at the blue edge of the emission spectra, which might offset the increase in fluorescence intensity caused by dissociation.

The pressure dependence of ΔG_{diss} permitted calculation of a standard volume change (ΔV_{diss}) of -50 mL/mol for the dissociation of FI from SCA 4-4-20. The reported value for ΔV of dissociation of rhodamine from the Bence-Jones dimer Mcg is in the range of -20 mL/mol (Herron et al., 1985). However, a ΔV of only -5 mL/mol has been found for the dissociation of FI from mAb 4-4-20 (Herron et al., 1986). The discrepancy in the two ΔV values for anti-FI antibodies is likely related to differences in the stability of the overall structures of SCA and mAb. Two explanations can be considered for these observations. First, the larger ΔV_{diss} for SCA results from the pressure-induced disruption of the FI binding site located at the interface between the two variable domains, with consequent FI dissociation. Such disruption of the binding site would not occur in mAb, where the presence of the constant domains prevents large-scale fluctuations of the variable domains. The second hypothesis proposes that the larger ΔV for FI-SCA dissociation is related to destabilization of the SCA structure upon release of the ligand, which would allow the unliganded protein to fluctuate among smaller volume conformations, whereas the structure of IgG would remain relatively rigid upon ligand dissociation. The first hypothesis is weakened by the fact that significant changes in the intrinsic fluorescence emission of liganded SCA occurred only about 1.6 kbar (Figure 6) whereas FI dissociation was observed at 1 kbar (Figure 3). Thus, the eventual conformational changes undergone by the liganded SCA molecule upon pressure occur at higher pressures than those necessary to promote ligand dissociation. Corroboration of the second hypothesis is based on the observation that FI stabilizes SCA 4-4-20 against pressure (Figure 6), supporting the view that the conformational fluctuations associated with the large standard volume of dissociation of FI-SCA occur as a consequence of ligand dissociation. Further evidence indicating that the primary effect of pressure on the FI-SCA complex is in promoting ligand dissociation instead of disrupting the FI binding site is the fact that dissociation of FI is dependent on protein concentration (Figures 2 and 3). If the primary effect of pressure were to dissociate the two variable domains, thus causing release of the FI ligand (*i.e.*, a first-order process), dissociation of FI should be unaffected by changing protein concentration.

Application of pressure up to 2.4 kbar does not promote direct changes on the tertiary structure of proteins such as protein unfolding (Weber & Drickamer, 1983; Weber, 1987). Therefore, the pressure-induced changes in the intrinsic SCA fluorescence in the unliganded state should be associated with conformational rearrangements that result in decreased volume of the protein. It might be possible that pressure induces dissociation of the two variable domains that constitute SCA 4-4-20, simulating the dissociation of a dimeric protein. However, the absence of a spectral red-shift of the intrinsic fluorescence emission prevents the conformation of the hypothesis (see Results). Thus, the nature of the conformational changes undergone by unliganded SCA 4-4-20 under pressure remains to be established.

Iodide quenching of bound FI revealed that, at the mAb site, FI was inaccessible to iodide while at the SCA site FI was accessible (Figure 7). This difference in accessibility of the ligand may account for the decrease of ~ 4 times in FI

affinity observed in the SCA molecule as compared to the corresponding mAb (Bedzyk et al., 1990). Differences in accommodation of the ligand in binding sites between the two molecules have been previously suggested by Tetin et al. (1992), who found significant differences between the CD spectra of liganded SCA and mAb 4-4-20.

Recent studies on the association of lysozyme with anti-lysozyme antibodies have proposed that formation of the antigen-antibody complex is enthalpically driven (Mariuzza & Poljak, 1993). On the other hand, an increase in entropy has been shown to play an important role in the association of FI with anti-FI antibodies (Herron et al., 1986). In the latter case, the entropic component derives from the favorable contribution of the hydrophobic effect (Tanford, 1980), partially offset by the unfavorable contribution of the reduction of vibrational motions associated with ligand binding (Sturtevant, 1977). In this work, we found that pressure-induced dissociation of FI from SCA 4-4-20 was strongly dependent on temperature (Figure 8). Similar effects of temperature have been observed by Müller et al.² for the dissociation of FI from SCA 4-4-20 in glycerol. The fact that FI dissociation increased with decreasing temperature suggested that binding of FI to SCA 4-4-20 occurred with a positive change in enthalpy, despite the overall significant negative change in free energy (ΔG). In fact, measurement of FI dissociation from SCA 4-4-20 upon decreasing temperature at atmospheric pressure that ΔH_{assn} is positive; *i.e.*, the association is enthalpically unfavorable (Figure 9). Formation of an antigen-antibody complex characterized by positive ΔH_{assn} has been previously reported for the reaction between anti-Rh blood group antibodies and Rh-positive erythrocytes (Green, 1982). To compensate for the unfavorable contribution of the enthalpic component, formation of the FI-SCA complex occurs with large positive ΔS (47 cal/kmol Figure 9). This value is larger than those reported for binding of FI to mAb 4-4-20, which were in the range of 26–32 cal/kmol (Herron et al., 1986). As noted above, the magnitude of the entropic term may be decreased by a reduction in motions of the ligand and protein structure upon binding; thus, the large ΔS_{assn} for FI binding to SCA relative to mAb 4-4-20 may reflect a less restrictive FI environment at the binding site. This is in line with the greater accessibility of FI to the hydrophilic quencher, iodide, when bound to SCA than to mAb 4-4-20 (Figure 7).

Collectively, the results presented in this study indicate that the SCA 4-4-20 structure presents significant differences relative to the original mAb 4-4-20 both at the level of the overall structure of the protein and at the level of the ligand binding site. SCA undergoes extensive stabilization upon FI binding, giving rise to a pronounced increase in the volume of the FI-antibody complex. Hapten-induced stabilization of the antibody conformation brings to the scene the idea of a "conformational tuning" induced by the ligand (Edmundson et al., 1984), which seems to specially characterize the association of FI to SCA 4-4-20.

ACKNOWLEDGMENT

We thank Dr. Gregorio Weber for the use of the spectrophotometer and for his insight and stimulating discussions. We also thank Dr. Sergio T. Ferreira for helpful suggestions and critical reading of the manuscript. Fluorescence measurements were performed at the Laboratory for Fluor-

² J. Müller, H. Frauenfelder, G. U. Nienhaus, S. Y. Tetin, and E. W. Voss, Jr. (1993), unpublished results.

rescence Dynamics (LFD) at the University of Illinois at Urbana—Champaign (UIUC). The LFD is supported jointly by the Division of Research Resources of the National Institutes of Health (RR03155-01) and the UIUC.

REFERENCES

- Bedzyk, W. D., Johnson, L. S., Riordan, G. S., & Voss, E. W., Jr. (1989) *J. Biol. Chem.* **264**, 1565–1569.
- Bedzyk, W. D., Weidner, K. M., Denzin, L. K., Johnson, L. S., Hardman, K. D., Pantoliano, M. W., Asel, E. D., & Voss, E. W., Jr. (1990) *J. Biol. Chem.* **265**, 18615–18620.
- Bird, R. E., Hardman, K. D., Jacobson, J. W., Johnson, S., Kaufman, B. M., Lee, S., Lee, T., Pope, S. H., Riordan, G. S., & Whitlow, M. (1988) *Science* **242**, 423–426.
- Chaudhary, V. K., Queen, C., Junghans, R. P., Waldmann, T. A., Fitzgerald, D. J., & Pastan, I. (1989) *Nature* **339**, 393–397.
- Coelho-Sampaio, T., Ferreira, S. T., Benaim, G., & Vieyra, A. (1991) *J. Biol. Chem.* **266**, 22266–22272.
- Denzin, L. K., Whitlow, M., & Voss, E. W., Jr. (1991) *J. Biol. Chem.* **266**, 14095–14103.
- Edmundson, A. B., Ely, K. R., & Herron, J. N. (1984) *Mol. Immunol.* **21**, 561–576.
- Glockshuber, R., Malia, M., Pfitzinger, I., & Plückthun, A. (1990) *Biochemistry* **29**, 1362–1367.
- Green, F. A. (1982) *Immunol. Commun.* **11**, 25–32.
- Herron, J. N. (1984) in *Fluorescein Hapten: An Immunological Probe* (Voss, E. W., Jr., Ed.) pp 49–76, CRC Press, Boca Raton, FL.
- Herron, J. N., Ely, K. R., & Edmundson, A. B. (1985) *Biochemistry* **24**, 3453–3459.
- Herron, J. N., Kranz, D. M., Jameson, D. M., & Voss, E. W., Jr. (1986) *Biochemistry* **25**, 4602–4609.
- Herron, J. N., He, X., Mason, M. L., & Voss, E. W., Jr. (1989) *Proteins: Struct., Funct., Genet.* **5**, 271–280.
- Howlett, J. R., Ismail, A. A., Armstrong, D. W., & Wong, P. T. (1992) *Biochim. Biophys. Acta* **1159**, 227–236.
- Huston, J. S., Levinson, D., Mudgett-Hunter, M., Tai, M.-S., Novotny, J., Margolies, M. N., Ridge, R. J., Bruccoleri, R. E., Haber, E., Crea, R., & Opperman, H. (1988) *Proc. Natl. Acad. Sci. U.S.A.* **85**, 5879–5883.
- Kranz, D. M., & Voss, E. W., Jr. (1981) *Mol. Immunol.* **18**, 889–898.
- Kranz, D. M., Herron, J. N., & Voss, E. W., Jr. (1982) *J. Biol. Chem.* **257**, 6987–6995.
- Kranz, D. M., Ballard, D. W., & Voss, E. W., Jr. (1983) *Mol. Immunol.* **20**, 1313–1322.
- Lakowicz, J. R. (1983) *Principles of Fluorescence Spectroscopy*, Plenum Press, New York.
- Li, T. M., Hook, J. W., III, Drickamer, H. G., & Weber, G. (1976a) *Biochemistry* **15**, 3205–3211.
- Li, T. M., Hook, J. W., III, Drickamer, H. G., & Weber, G. (1976b) *Biochemistry* **15**, 5571–5580.
- Mariuzza, R. A., & Poljak, R. J. (1993) *Curr. Opin. Immunol.* **5**, 50–55.
- Masson, P., & Balny, C. (1990) *Biochim. Biophys. Acta* **1159**, 223–231.
- Paladini, A. A., & Weber, G. (1981) *Biochemistry* **20**, 2587–2593.
- Reinitz, D. M., & Voss, E. W., Jr. (1984) *Mol. Immunol.* **21**, 775–784.
- Ronzani, N., Stephan, L., & Hasselbach, W. (1991) *Eur. J. Biochem.* **201**, 265–271.
- Silva, J. L., Miles, E. W., & Weber, G. (1986) *Biochemistry* **25**, 5780–5786.
- Sturtevant, J. M. (1977) *Proc. Natl. Acad. Sci. U.S.A.* **74**, 2236–2240.
- Swindlehurst, C. A., & Voss, E. W., Jr. (1991) *Biophys. J.* **59**, 619–628.
- Tanford, C. (1980) *The Hydrophobic Effect*, 2nd ed., Wiley, New York.
- Tetin, S. Y., Mantulin, W. W., Denzin, L. K., Weidner, K. M., & Voss, E. W., Jr. (1992) *Biochemistry* **31**, 12029–12034.
- Thompson, R. B., & Lakowicz, J. R. (1984) *Biochemistry* **23**, 3411–3417.
- Weber, G. (1987) *NATO ASI Ser., Ser. C* **197**, 401–420.
- Weber, G. (1992) *Protein Interactions*, Chapman & Hall, New York.
- Weber, G., & Drickamer, H. G. (1983) *Q. Rev. Biophys.* **16**, 89–112.
- Yokota, T., Milenic, D. E., Whitlow, M., & Schlom, J. (1992) *Cancer Res.* **52**, 3402–3408.